Intrinsic Neuronal Determinants Locally Regulate Extrasynaptic and Synaptic Growth at the Adult Neuromuscular Junction

Pico Caroni, Ludwig Aigner, and Corinna Schneider

Friedrich Miescher Institute, CH-4002 Basel, Switzerland

Abstract. Long-term functional plasticity in the nervous system can involve structural changes in terminal arborization and synaptic connections. To determine whether the differential expression of intrinsic neuronal determinants affects structural plasticity, we produced and analyzed transgenic mice overexpressing the cytosolic proteins cortical cytoskeleton–associated protein 23 (CAP-23) and growth-associated protein 43 (GAP-43) in adult neurons.

Like GAP-43, CAP-23 was downregulated in mouse motor nerves and neuromuscular junctions during the second postnatal week and reexpressed during regeneration. In transgenic mice, the expression of either protein in adult motoneurons induced spontaneous and greatly potentiated stimulus-induced nerve sprouting at the neuromuscular junction. This sprouting had trans-

gene-specific features, with CAP-23 inducing longer, but less numerous sprouts than GAP-43. Crossing of the transgenic mice led to dramatic potentiation of the sprout-inducing activities of GAP-43 and CAP-23, indicating that these related proteins have complementary and synergistic activities. In addition to ultraterminal sprouting, substantial growth of synaptic structures was induced. Experiments with pre- and postsynaptic toxins revealed that in the presence of GAP-43 or CAP-23, sprouting was stimulated by a mechanism that responds to reduced transmitter release and may be independent of postsynaptic activation.

These results demonstrate the importance of intrinsic determinants in structural plasticity and provide an experimental approach to study its role in nervous system function.

THE formation of neuronal connections involves a sequence of distinct stages in axonal growth, i.e., long-distance elongation, growth of collaterals to reach the target region, and innervation of target cells. Terminal arborization initiates the final phase of the innervation process. This dynamic process provides the presynaptic substrate for the formation and activity-sensitive refinement of synaptic connections during development. In the adult, it can be reactivated by local deafferentation, leading to sprouting and reinnervation (e.g., Brown, 1984). In addition, there is now substantial evidence supporting the view that the dramatic extent of learning-induced functional plasticity in the adult vertebrate nervous system also involves local changes in terminal arborization and synaptic connections (see e.g., Bailey et al., 1994; Darian-Smith and Gilbert, 1994; Das and Gilbert, 1995). Because of the fact that terminal arborization plays such a central role in nervous system plasticity, it is of great interest to define the mechanisms that promote and regulate this process.

One factor that affects nerve sprouting and terminal arborization is the expression of competence conferring com-

ponents in responding neurons (Skene, 1989; Woolf et al., 1992; Aigner et al., 1995). These include specific receptors for extracellular signals, as well as corresponding signal transduction and growth machinery to translate defined signals into local growth. The neural protein kinase C (PKC)[1] substrate growth-associated protein 43 (GAP-43) is a cytosolic growth cone and nerve terminal protein that promotes local nerve growth and appears to belong to the latter category (for reviews see Benowitz and Routtenberg, 1987; Skene, 1989; Liu and Storm, 1990). This axonal protein is expressed during nerve elongation and terminal arborization and is usually downregulated when synaptic rearrangements are completed, but its expression is selectively maintained in defined types of neurons in the adult. Although GAP-43 is not required for nerve growth (Strittmatter et al., 1995), the existence of a strong correlation between its expression in the developing and adult nervous system and competence for nerve sprouting suggests that GAP-43 may potentiate local nerve growth. This view received support from the recent demonstration that over-

Address all correspondence to Pico Caroni, Friedrich Miescher Institute, P.O. Box 2543, CH-4002 Basel, Switzerland. Tel.: 41-51-6973727. Fax: 41-61-6973976. E-mail: caroni@fmi.ch

1. *Abbreviations used in this paper*: AChR, acetylcholine receptor; Bot-A, Botulinum toxin-A; CAP, cortical cytoskeleton–associated protein; GAP, growth-associated protein; MARCKS, myristoylated alanine-rich C kinase substrate; PKC, protein kinase C.

expression of GAP-43 in the neurons of adult transgenic mice leads to spontaneous and greatly potentiates induced nerve sprouting (Aigner et al., 1995). The results with GAP-43 have raised the possibility that the expression of growth- and plasticity-associated proteins in neurons may promote their growth responses to local signals. This hypothesis predicts that intrinsic growth–promoting properties are not restricted to GAP-43 and that neurons may express diverse sets of plasticity-promoting proteins. Such proteins would act downstream of signal transduction pathways initiated by extracellular ligands to promote the translation of receptor activation into cytoskeletal rearrangements and local growth. Expression of particular combinations of these proteins may affect the intrinsic competence of neurons for local structural plasticity.

One protein that may be functionally related to GAP-43 is the cortical cytoskeleton-associated protein CAP-23 (Widmer and Caroni, 1990). Although GAP-43 and CAP-23 do not have homologous sequences, they share several characteristic biochemical properties. These include: 1) Both proteins bind calmodulin and are phosphorylated by PKC in a mutually exclusive manner (Liu and Storm, 1990; Maekawa et al., 1993, 1994); 2) they have highly hydrophilic sequences, the same type of unusual amino acid composition rich in Ala, Pro, Lys, and Glu, and very little secondary structure (Skene, 1989; Widmer and Caroni, 1990); 3) both are acylated proteins (GAP-43 is palmitoylated [Skene and Virag, 1989], whereas CAP-23 is myristoylated [Maekawa et al., 1994]) that colocalize at unique punctate structures at the cell membrane (Wiederkehr, A., and P. Caroni, manuscript submitted for publication) and interact with the cortical cytoskeleton (Meiri and Gordon-Weeks, 1990; Moss et al., 1990; Widmer and Caroni, 1990); and 4) their expression is highly regulated and peaks during development of the nervous system, when they can represent up to 0.2% (GAP-43) and 0.8% (CAP-23) of total brain protein (Skene, 1989; Widmer and Caroni, 1990; Maekawa et al., 1993). In addition, GAP-43 (Caroni and Becker, 1992) and CAP-23 (see Fig. 1) are downregulated and reinduced with comparable kinetics in spinal motoneurons, and they induce the same type of characteristic surface activities in transfected cells (Wiederkehr, A., and P. Caroni, manuscript submitted for publication).

To determine whether CAP-23 has sprout-promoting activity and to explore the possibility that neurons may express growth-promoting proteins with overlapping and/or synergistic activities, we generated transgenic mice that constitutively expressed CAP-23 in adult neurons. Like GAP-43–overexpressing mice, these mice displayed spontaneous and greatly potentiated induced nerve sprouting at the neuromuscular junction. However, the sprouting patterns in the presence of GAP-43 or CAP-23 were different, and double-transgenic mice expressing both proteins in motoneurons displayed dramatic quantitative and qualitative potentiation of sprouting. We then carried out experiments aimed at defining the properties and regulation of the structural plasticity promoted by these growth-associated proteins. These experiments revealed that: 1) Alterations in both nerve growth and postsynaptic structures were induced at the neuromuscular junction of the transgenic mice; 2) growth-promoting pathways are rapidly activated by reduced transmitter release, possibly independent of muscle nicotinic acetylcholine receptor (AChR) activation; and 3) paralysis promotes sprout elongation.

Materials and Methods

Generation of CAP-23 Transgenic Mice

The Thy1.2-based expression cassette was as described (Aigner et al., 1995; see also Vidal et al., 1990). It drives transgene expression specifically in postnatal mouse neurons, including spinal motoneurons. A description of its expression properties can be found elsewhere (Caroni, 1996). cDNA coding for chick CAP-23 (Widmer and Caroni, 1990) was cloned into the Thy1 expression cassette. To avoid possible regulation of CAP-23 mRNA stability or translation due to regulatory sequences in the untranslated regions, the cDNA sequences only contained 7 nucleotides of 5'-, and 10 nucleotides of 3'-untranslated region. Seven independent transgenic lines were generated. Of these, three lines were excluded from further analysis because of low expression of the transgene, as assayed by immunoblots of brain homogenates and by immunocytochemistry on skeletal muscle sections (motor nerve expression). To minimize possible effects due to differences in genetic background, all lines of GAP-43– and CAP-23–overexpressing mice were bred into C57Bl6 mice for at least five generations. Inbreeding did not appear to affect spontaneous nerve sprouting in the transgenic mice. However, because of better breeding results, most experiments were carried out in outbred Balb/C × C57Bl6 mice. A survey of mouse tissues revealed no further expression outside the nervous system. In particular, we found no transgene expression in innervated or denervated muscle, nor in intramuscular Schwann cells (data not shown, but see Aigner et al., 1995). In the nervous system, we detected prominent expression in a diverse range of neuronal types in the peripheral nervous system and central nervous system (see Fig. 2 A), but no expression in GFAP-positive astrocytes, peripheral nerve Schwann cells, terminal Schwann cells at the neuromuscular junction, or GalC-positive oligodendrocytes (data not shown). The transgenic lines were designated as follows: CAP-23(2, 11, 13, 17), mice expressing chick CAP-23; and GAP-43(wt2, wt3), mice expressing chick GAP-43 (Aigner et al., 1995).

Detection of mRNAs and Proteins

In situ hybridization for chick CAP-23 was carried out on frozen sections with a digoxigenin-labeled cRNA probe, as described (Schaeren-Wiemers and Gerfin-Moser, 1993; Arber and Caroni, 1995). Total RNA was isolated and analyzed on Northern blots with digoxigenin-labeled riboprobes, as described (Arber et al., 1994). A rat cDNA coding for the γ-subunit of the acetylcholine receptor was a kind gift from A. Buonanno (National Institutes of Health, Bethesda, MD). For immunoblots, brains were homogenized in SDS-PAGE sample buffer, protein contents were determined, and 40 μg of protein were loaded per slot. CAP-23 was visualized with either monoclonal antibody 15C1 (Widmer and Caroni, 1990), which specifically detects chick but not mouse CAP-23, or with a rabbit antiserum to the carboxyl-terminal residues VASSEQSVAVKE of rat and mouse neuronal acidic protein 22 (NAP-22). (This antiserum does not crossreact with chick CAP-23.) NAP-22 (Maekawa et al., 1993) is the rat homologue of CAP-23. (The correct carboxyl-terminal sequence of chick CAP-23 is 171-AETKSEVAPASDSKPSSPSSKETVAATAAPSSTA-KASDPSAPPEEAKPSEAPATNSDTTIAVQD-234; due to two frameshift errors in the 3'-end sequence of the cDNA, the original sequence [Widmer and Caroni, 1990] contained two translation errors.) GAP-43 was visualized as described (Aigner et al., 1995). Immunocytochemistry was performed on 12-μm cryostat sections of 4%-formaldehyde–fixed tissues. Antibodies were applied in PBS with 0.5% NP-40 (Sigma Chemical Co., St. Louis, MO) and 5% BSA as described (Widmer and Caroni, 1990). Monoclonal antibody supernatants were diluted 1:100. Neurofilament-160 was detected with a specific monoclonal antibody (Sigma Chemical Co.). Rhodamine-α-bungarotoxin was from Molecular Probes (Eugene, OR). Bound antibodies were visualized with Biotin-conjugated second antibodies, followed by Lucifer yellow–conjugated streptavidin, and with rhodamine-conjugated second antibodies. (All secondary antibody reagents were from Molecular Probes.) Postsynaptic neuromuscular junction configurations were visualized by labeling whole-mount preparations of gluteus muscle with RITC–α-bungarotoxin. All procedures were carried out at 4°C. Briefly, muscles were incubated for 5 h in L15/PBS (1:2)

with 1 µg/ml of RITC–α-bungarotoxin, rinsed with PBS, and fixed overnight with 2% paraformaldehyde in phosphate buffer (pH 7.4). Groups of one to five muscle fibers were then dissected in water and mounted in airvol.

Lesion Protocols

For most experiments, local paralysis was induced by a single subcutaneous injection of 1 pg of purified Botulinum toxin A (kind gift of C. Montecucco, Pavia, Italy, and S. Catsicas, Geneva, Switzerland) over the right gluteus maximus or gastrocnemius of 4–6-wk-old mice. For 3-wk paralysis experiments, a second injection of 0.8 pg Botulinum toxin-A (Bot-A) was applied at 10 d. In an alternative protocol, paralysis was induced by local applications of α-bungarotoxin (Sigma Chemical Co.; in PBS, with 0.1% BSA; 1 µg on the first day, and then 0.5 µg every second day) onto the gastrocnemius. Because of the potential difficulties in inducing persistent paralysis with α-bungarotoxin, we also carried out a series of experiments in which a priming injection (1 µg) was followed by daily applications of 0.35 µg of the toxin. In these experiments, absence of the toe-spreading reflex was also verified daily. A third procedure consisted in applying tetrodotoxin (Sigma Chemical Co.; 1.2 µg per day in DME with 0.1% BSA) through a sciatic nerve cuff supplied by an osmotic minipump (ALZET model 1007D; Alza Corp., Palo Alto, CA), according to a published procedure (Witzemann et al., 1991). Depending on the paralysis protocol, paralysis was obvious 5–24 h after the beginning of the treatment and was verified by the missing toe-spreading reflex (gastrocnemius), as described (Witzemann et al., 1991). Possibly because of technical difficulties in obtaining a tight seal at the cuff site, in most tetrodotoxin-treated animals, paralysis signs became less obvious after 3–4 d. For crush experiments, mice were anesthetized and the right sciatic nerve was exposed at mid-thigh level and crushed, as described (Aigner et al., 1995).

Detection and Analysis of Sprouting

Intramuscular nerves and neuromuscular junctions were visualized on 50-µm cryostat sections of gastrocnemius and gluteus maximus muscle, as described (Pestronk and Drachman, 1978a; Caroni et al., 1994). For the unambiguous identification of sprouts, only nerve profiles longer than 5 µm that clearly extended beyond the endplate area (ultraterminal sprouts) were included in the analysis. At least 300 endplates per animal were analyzed as described (Aigner et al., 1995). Values are averages ±SEM. For statistical analysis, the Mann–Whitney U test was applied. To provide a measure of the total length of the sprouts in a given muscle, the lengths of all ultraterminal sprouts and the total number of neuromuscular synapses (including all neuromuscular junctions in a given field, i.e., those with and without sprouts) in randomly selected fields were summed and normalized to 500 neuromuscular junctions (i.e., total length of sprouts in all randomly selected fields, divided by total number of neuromuscular synapses in the same fields, times 500). Branch-points per endplate included every silver (neurofilament)–positive side-branch of >4 µm within the esterase-positive synaptic region. These therefore reflect both ultraterminal sprouting and the extent of terminal branching at the synapse. Not included were branch-points from the preterminal region of the motor nerve and from ultraterminal sprouts. Regenerative nerve growth 64 h after sciatic nerve crush was analyzed on longitudinal 12-µm cryostat sections by counting the number of neurofilament-160-positive profiles 1–2 and 5–6 mm distal from the crush site, as described (Aigner et al., 1995). Synaptic areas were estimated on RITC–α-bungarotoxin–labeled whole-mount preparations of 5–6-wk gluteus maximus muscles with NIH Image 1.4 software. Only endplates with most of their apparent overall outlines in the plane of focus were included in the analysis. The values are averages ±SEM of 75 endplates each (3 animals, 25 endplates each).
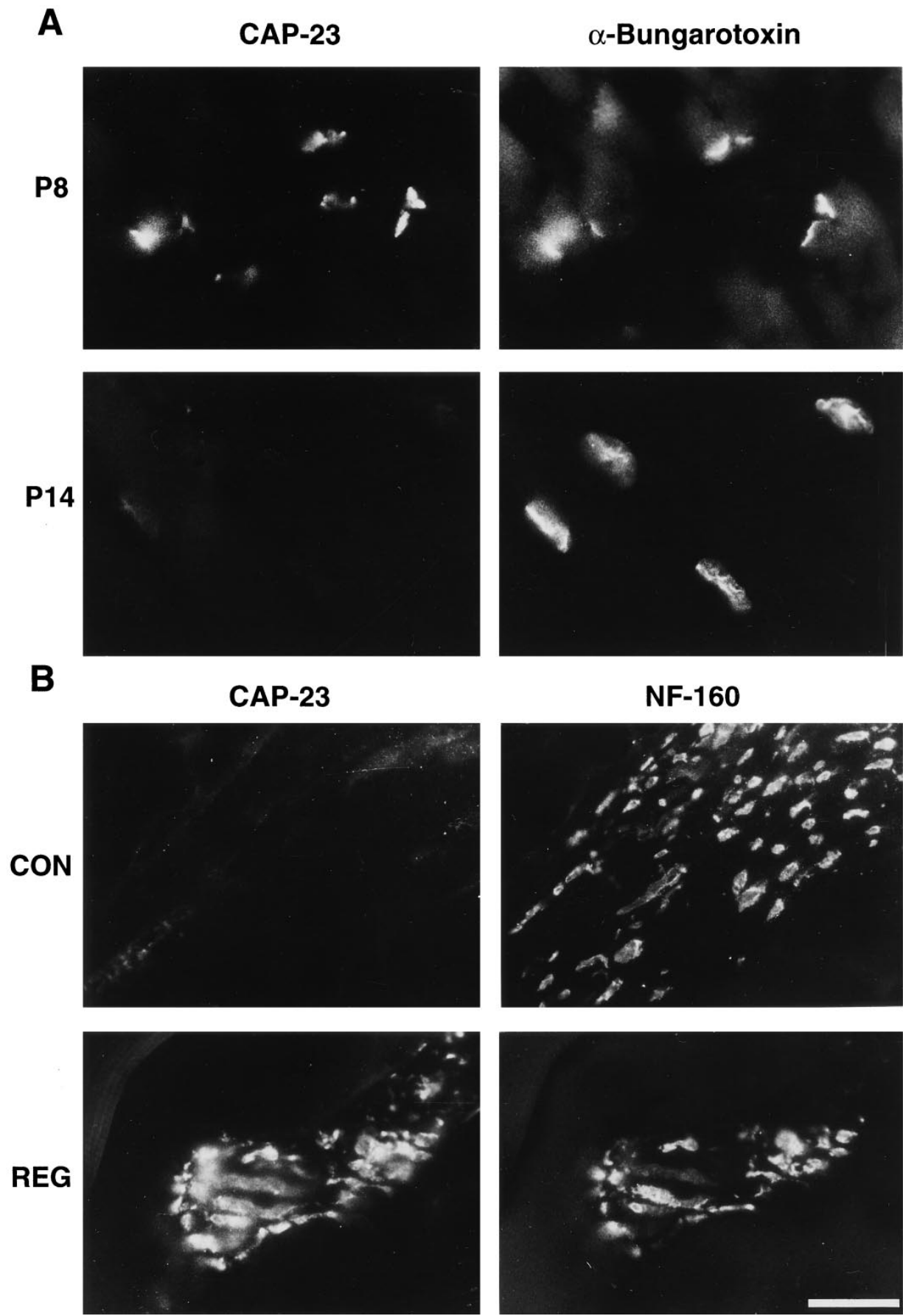
Results

Parallel Regulation of GAP-43 and CAP-23 in Motoneurons and at the Neuromuscular Junction

In 2–3-d chick embryos, CAP-23 is expressed at high levels in most cells (Widmer and Caroni, 1990). Subsequently, expression becomes restricted to the nervous system, where it peaks around embryonic day 17 (Widmer and Caroni, 1990). In the adult, expression is lower and is mainly restricted to certain types of neurons. To better define the

time course of CAP-23 downregulation and to determine whether its expression is induced upon nerve lesion, we carried out appropriate experiments in the developing and adult mouse neuromuscular system. Intramuscular nerve and neuromuscular junction CAP-23 immunoreactivity did not change significantly between birth and postnatal day (P) 8 (data not shown). Subsequently, as shown in Fig. 1 *A*, it was downregulated between postnatal days 8 and 14, when no CAP-23 immunoreactivity could be detected at most neuromuscular junctions. Thus, like GAP-43 (Caroni and Becker, 1992), downregulation of CAP-23 in this system coincides with the time when muscle stops growing by the addition of new fibers and with the final phase of synapse elimination. Fig. 1 *B* shows nerve-associated CAP-23 immunoreactivity in adult gastrocnemius muscle before and 10 d after sciatic nerve crush. CAP-23 was not detectable in adult intramuscular nerves, where it was reinduced during regeneration. Therefore, like GAP-43 (Skene, 1989), CAP-23 is reexpressed in regenerating peripheral nerves.

CAP-23–overexpressing Mice Exhibit Spontaneous and Potentiated Induced Nerve Sprouting at the Neuromuscular Junction

To determine whether the presence of CAP-23 in adult nerves affects nerve sprouting, we produced CAP-23–overexpressing transgenic mice. We used the same mouse Thy1.2 expression cassette that had been used to generate GAP-43–overexpressing mice, and that leads to neuron-specific expression of transgene, starting around P5–10 (Aigner et al., 1995). Chick and mouse CAP-23 are highly homologous but can be distinguished with specific antibodies. Therefore, to allow for independent detection of endogenous and transgenic CAP-23, we used chick CAP-23 as a transgene. Four independent transgenic lines with substantial expression levels in spinal motoneurons were selected for further analysis. These will be designated in the following as CAP-23(C11), CAP-23(C2), CAP-23(C17), and CAP-23(C13). As shown in Fig. 2 *A*, transgenic CAP-23 was expressed in several types of adult neurons, including spinal motoneurons. The data shown in the figure are from a CAP-23(C11) mouse. Although the other transgenic lines displayed similar widespread expression, with strong signals in spinal motoneurons, specific differences were noticed. However, due to the focus of this study, these differences will not be discussed here. Fig. 2 *B* shows that transgene levels in homogenates of adult mouse brain were comparable to maximal levels reached for endogenous chick CAP-23. The figure also shows that monoclonal antibody 15C1 does not crossreact with mouse CAP-23. Finally, Fig. 2 *C* demonstrates that prominent levels of chick CAP-23 immunoreactivity could be detected at the adult neuromuscular junction of CAP-23(C11) mice, whereas from P15 on endogenous CAP-23 (Fig. 2 *C*) and GAP-43 (not shown) were undetectable. Comparable results were obtained for the other transgenic lines included in the analysis, with highest signals in CAP-23(C2) and lowest signals in CAP-23(C13) mice. In situ hybridization and Northern blot analysis failed to reveal any transgene expression in muscle (data not shown). In addition, intramuscular nerve and neuromuscular junction trans-

A

CAP-23   α-Bungarotoxin

P8

P14

B

CAP-23   NF-160

CON

REG

gene immunoreactivity was abolished 3 d after denervation. Taken together, these results show that, as already described for the corresponding GAP-43–overexpressing mice (Aigner et al., 1995), transgene expression was restricted to neurons and did not activate the expression of endogenous CAP-23 or GAP-43.

Analysis of neuromuscular innervation patterns with a combined silver-esterase reaction revealed prominent ultraterminal sprouting in CAP-23–overexpressing mice (Fig. 3, *A* and *C*). Quantitative analysis revealed that the values for the fraction of neuromuscular junctions with ultraterminal sprouts and the total length of ultraterminal sprouts per muscle were comparable to those detected in GAP-43–overexpressing mice (see Fig. 5 *B*) and higher than those induced in nontransgenic mice by paralysis with Bot-A (Brown, 1984) (Fig. 3 *C*). Like in GAP-43–overexpressing mice (Aigner et al., 1995), sprouting extents and apparent local expression levels as detected by CAP-23 immunocytochemistry were correlated. Accordingly, CAP-23(C11) and CAP-23(C2) mice exhibited substantially more sprouting than CAP-23(C17) and CAP-23(C13) mice (data not shown). Although sprouting patterns were different, substantial sprouting was detected in all analyzed muscles, including lateral and medial gastrocnemius, extensor digitorum longus, gluteus maximus, soleus, and diaphragm. Strongest sprouting was detected in gluteus maximus and lateral gastrocnemius, and most of the analysis was carried out in the gluteus muscle. Detailed comparison with GAP-43–overexpressing mice revealed the following differences: (*a*) In the presence of CAP-23, sprouts were on average about three to four times longer (Fig. 3 *D*; $P < 0.05$); (*b*) CAP-23–overexpressing mice had fewer sprouts per endplate (about half; Fig. 3 *D*; $P < 0.05$); and (*c*) growth cone-like enlargements were detected in ~30% of GAP-43–induced sprouts but in <5% of those induced in the presence of CAP-23. These different qualitative features of the sprouting patterns in GAP-43– and CAP-23–overexpressing mice were consistently detected in several independent transgenic lines. As for sprouting in the presence of GAP-43, no signs of functional denervation could be detected in the muscles of CAP-23–overexpressing mice. Thus, mRNAs that are induced in skeletal muscle by denervation or paralysis in the presence of Bot-A were not induced in any of the CAP-23–overexpressing mice (Fig. 3 *B*; further denervation-sensitive mRNAs that were not induced in CAP-23–overexpressing mice included those coding for MLP [Arber et al., 1994] and N-CAM). In addition, intracellular recordings of spontaneous and nerve-induced postsynaptic potentials in nerve-muscle explants failed to reveal abnormalities in evoked potentials, or in the amplitude of miniature endplate potentials (data not shown). Therefore, the presence of CAP-23 in motor nerves and at their synaptic endings is sufficient to induce a substantial ultraterminal sprouting reaction in the absence of any signs of functional denervation, indicating that, like GAP-43, CAP-23 promotes spontaneous nerve sprouting at the neuromuscular junction.

To determine whether the presence of CAP-23 potentiates induced nerve sprouting, thus producing a gain-of-function phenotype with respect to this local nerve growth reaction, we induced local paralysis with the presynaptically acting toxin-A from *Clostridium botulinum* (Brown, 1984). In preliminary experiments we verified that, as for GAP-43, muscle paralysis in the presence of Bot-A does not induce significant CAP-23 immunoreactivity in motor nerves or at the neuromuscular junction (data not shown), indicating that neither GAP-43 nor CAP-23 are required for nerve sprouting to occur. In further control experiments with decreasing doses of Bot-A, we determined that the sensitivity to Bot-A–induced paralysis was, if anything, higher in nontransgenic than in transgenic mice. We then analyzed nerve sprouting in 8- and 21-d-paralyzed muscles of nontransgenic and CAP-23–overexpressing mice. As shown in Fig. 4, *A* and *C*, toxin-induced sprouting was greatly potentiated in the presence of CAP-23. Significantly, instead of reducing the difference between nontransgenic and CAP-23–overexpressing mice, 3-wk paralysis augmented it, leading to dramatic sprouting extents and lengths in the presence of CAP-23 (Fig. 4 *C*). These results indicate that the presence of CAP-23 can promote sustained sprouting under favorable local conditions. They also indicate that CAP-23 must be operating through an intrinsic mechanism distinct from reduced trasmitter release.

In an independent test for the effects of CAP-23 on induced nerve sprouting, we analyzed short-term nerve growth induced by sciatic nerve crush. In this experimental paradigm, sprouting of axons into the distal section of the lesioned nerve is assayed at a time (64 h after lesion) when neurofilament-positive material from degenerating nerves has been largely removed, and lesion-induced CAP-23 and GAP-43 have not yet reached the crush site. As shown in Fig. 4 *B*, and in further analogy to GAP-43–overexpressing mice, the presence of CAP-23 significantly promoted this form of regenerative sprouting. In contrast, reinnervation of gastrocnemius muscle 8–11 d after the crush was not obviously faster in transgenic mice (data not shown, but see Aigner et al., 1995, for reinnervation data in GAP-43–overexpressing mice).

Figure 1. Expression of CAP-23 in mouse motor nerves and at the neuromuscular junction. (*A*) At the neuromuscular junction, CAP-23 immunoreactivity is downregulated during the second postnatal week. The figure shows double-labeling immunocytochemistry of cryostat sections from formaldehyde-fixed gluteus maximus muscle (equivalent photographic exposures). To visualize neuromuscular junctions, the sections were counterstained with RITC–α-bungarotoxin. CAP-23 immunoreactivity was well detectable at P8 and nearly undetectable at P14. In parallel experiments, a combination of α-bungarotoxin and antibody to neurofilament-160 labeled all CAP-23–positive structures (data not shown), suggesting that in postnatal muscles, CAP-23 expression was restricted to intramuscular nerves. (*B*) CAP-23 is reexpressed in regenerating intramuscular nerves in the adult. Double-labeling immunocytochemistry of gastrocnemius sections from a control (*CON*) and a mouse 10 d after mid-thigh level crush of the sciatic nerve (*REG*). Note that neurofilament-160 (*NF-160*)–positive nerves do not express CAP-23 in the adult but reexpress this protein during regeneration. These findings indicate that CAP-23 is a growth-associated protein of motor nerves. Bar, 23 μm.
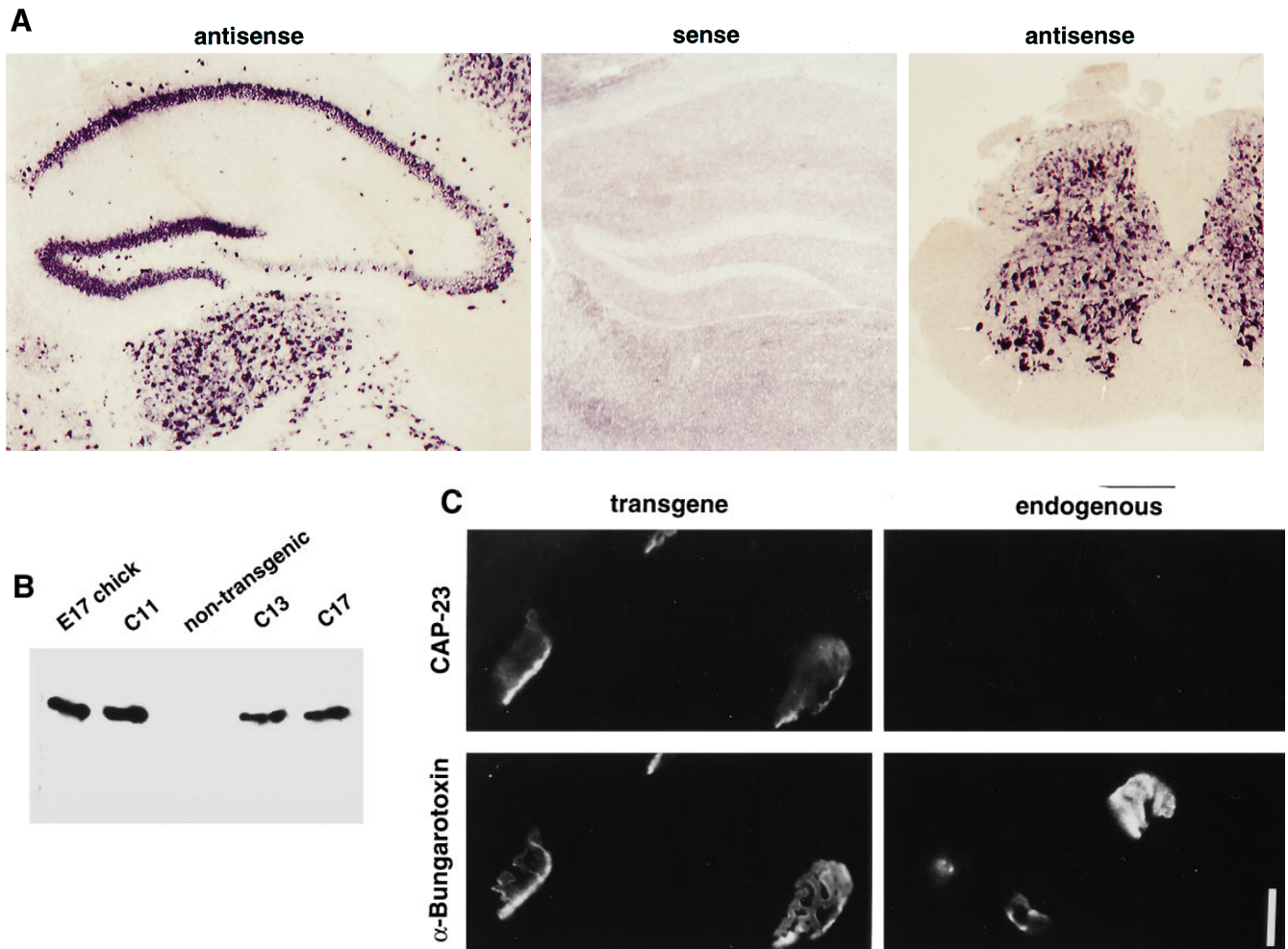
Figure 2. A mouse Thy1.2-based expression cassette drives expression of transgenic chick CAP-23 in adult mouse neurons, including spinal motoneurons. (*A*) Neuronal expression of chick CAP-23 transgene. In situ hybridization of adult mouse (line CAP-23[C11]) brain and spinal cord cryostat sections with digoxigenin-labeled chick CAP-23 cRNA. (*Left*) Strong transgene expression was detected in several neuronal types in the hippocampal formation (e.g., dentate gyrus granule cells, hilar cells, CA1; low in CA3) and in thalamic nuclei. No signal was detected with a corresponding sense probe (*center*). (*Right*) Strong transgene expression in spinal cord neurons (lumbar level), including large ventral horn motoneurons (*arrows*). Note absence of signal in the white matter (oligodendrocytes, astrocytes). (*B*) Transgene expression levels in adult mouse brain were comparable to those detected for endogenous CAP-23 in E17 chick brain, when levels of this protein are maximal. The immunoblot of brain homogenate fractions (40 μg of protein) was probed with monoclonal antibody 15C1, which specifically detects chick, but not mouse (nontransgenic sample) CAP-23. The transgenic lines were CAP-23(C11), CAP-23(C13), and CAP-23(C17). (*C*) Detection of transgenic, but not endogenous CAP-23 at the neuromuscular junction of a CAP-23(C11) transgenic mouse. Double-labeling immunocytochemistry for CAP-23 and α-bungarotoxin. (*Left*) Section reacted with monoclonal antibody 15C1. (*Right*) Section reacted with antiserum against carboxyl-terminal sequence from mouse CAP-23 (no crossreactivity with chick CAP-23). Bar, 45 μm.

Synergism between CAP-23 and GAP-43 in the Induction of Local Nerve Growth

As shown in the previous sections, the patterns of ultraterminal sprouting at the neuromuscular junction of GAP-43– and CAP-23–overexpressing mice displayed consistent differences, and both proteins are expressed in motor nerves during development and regeneration. To determine whether GAP-43 and CAP-23 may have synergistic activities on nerve sprouting, we analyzed offsprings of transgenic mice crossings. Mice transgenic for GAP-43 and CAP-23 expressed both transgenes at the neuromuscular junction (data not shown). As shown in Fig. 5, *A* and *B*, this resulted in dramatic potentiation of nerve sprouting in untreated animals, with long and numerous sprouts that

were detected at essentially all neuromuscular junctions. Analysis of activity-sensitive muscle mRNAs (Fig. 5 *C*) and of nerve muscle explants (data not shown) established that this remarkable sprouting activity was not accompanied by detectable signs of neuromuscular inactivation. In control experiments, in mice homozygous for the GAP-43 (Fig. 5 *B*) or CAP-23 (data not shown) transgene, nerve sprouting was comparable to that detected in corresponding heterozygous mice, indicating that in these mice elevating transgene levels did not lead to potentiation of sprouting. We then determined whether the presence of both transgenes also potentiated induced sprouting. Double-transgenic mice displayed detectable, but comparatively modest potentiation of crush-induced sprouting
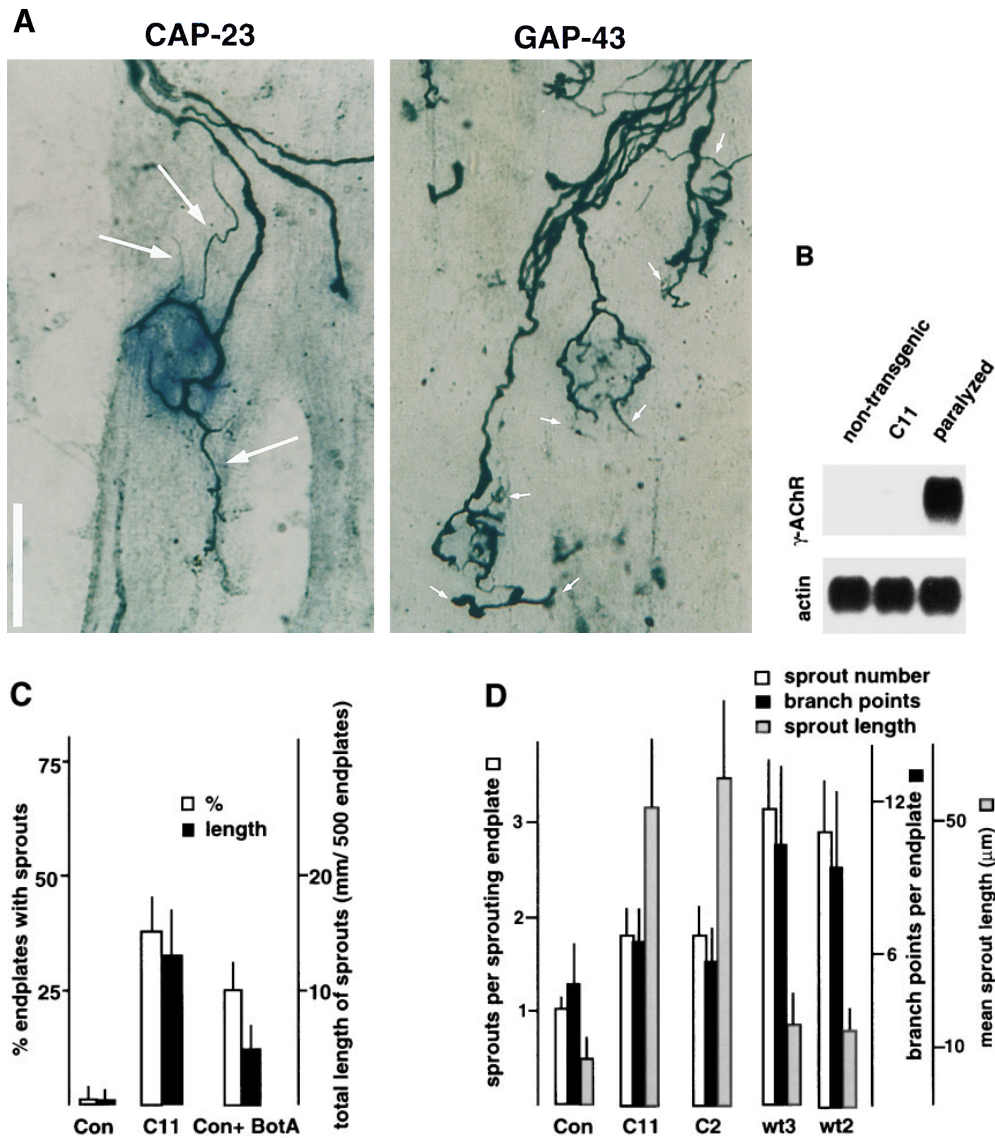
Figure 3. Neuromuscular junctions of CAP-23–overexpressing mice exhibit spontaneous nerve sprouting, with features distinct from those induced by GAP-43. Data are from 4–6-wk-old mice; gluteus maximus muscle. (*A*) Ultraterminal nerve sprouting in a CAP-23(C11) and a GAP-43(wt3) mouse. The combined silver-esterase reaction visualizes nerves (*black*) and acetylcholine esterase reaction product (*blue*; delimiting synaptic area). Note long ultraterminal sprouts in the presence of CAP-23 (*arrows*) and shorter sprouts (*arrows*; sprout at the bottom with growth cone structures) in the presence of GAP-43. (*B*) Contents of denervation-sensitive mRNA (γ-subunit of AChR) in skeletal muscle of nontransgenic and CAP-23(C11) mouse. As in nontransgenic animals, the gluteus of CAP-23(C11) mice did not express genes induced by the absence of electrical activation (e.g., Bot-A–induced paralysis [8 d; paralyzed]). (*C*) Quantitative analysis of ultraterminal sprouting in nontransgenic and CAP-23(C11) mice; comparison with the sprouting reaction induced in the same type of muscle by local paralysis (8 d) with Bot-A. $N = 8$. (*D*) Quantitative analysis of nerve sprouting patterns at the neuromuscular junction of nontransgenic (*Con*), CAP-23(C11), CAP-23(C2), GAP-43(wt3), and GAP-43(wt2) mice. Branch points per endplate: silver-stained processes; sprouting and nonsprouting endplates included. For a description of the sampling and analysis procedures, see Materials and Methods. Note distinct features of sprouting in the presence of CAP-23 (longer, less numerous sprouts) and GAP-43 (high number of branching points per endplate). Also note that "% of endplates with sprouts," "total length of sprouts," "mean sprout length," and "number of sprouts per sprouting endplate" refer to extrasynaptic branches, whereas "branch points per endplate" is a measure for branching within the endplate region, thus including intra- and ultraterminal growth. $N = 5$. Bar, 57 μm.

(data not shown). In contrast, the extent and pattern of Bot-A–induced growth at the neuromuscular junction were dramatically affected by the presence of both transgenes (Fig. 5 *D*). In addition, double-transgenic mice displayed a dramatic increase in the density of nerve processes at and in the immediate vicinity of paralyzed neuromuscular junctions. Therefore, the presence of both GAP-43 and CAP-23 at the neuromuscular junction leads to quantitative potentiation and qualitative alterations in paralysis-induced sprouting.

Synaptic and Extrasynaptic Growth in GAP-43 (or CAP-23)–overexpressing Mice

The demonstration of similar and synergistic activities of GAP-43 and CAP-23 on nerve sprouting at the adult neuromuscular junction strongly supports the notion that local nerve growth is affected by the presence of intrinsic growth-promoting components in neuronal processes. These findings lead to questions about the range of the structural alterations induced by the presence of these growth-promoting proteins and the signaling mechanisms that promote this type of growth. To begin to address the question of whether these proteins also promote alterations in synaptic structures, we visualized the distribution of acetylcholine receptors (AChRs) in RITC–α-bungarotoxin–labeled whole-mount muscle preparations. This revealed a substantial increase in the density of synaptic structures at the neuromuscular junction of CAP-23– (Fig. 6 *A*) and GAP-43–overexpressing (Fig. 6 *B*) mice. Quanti-
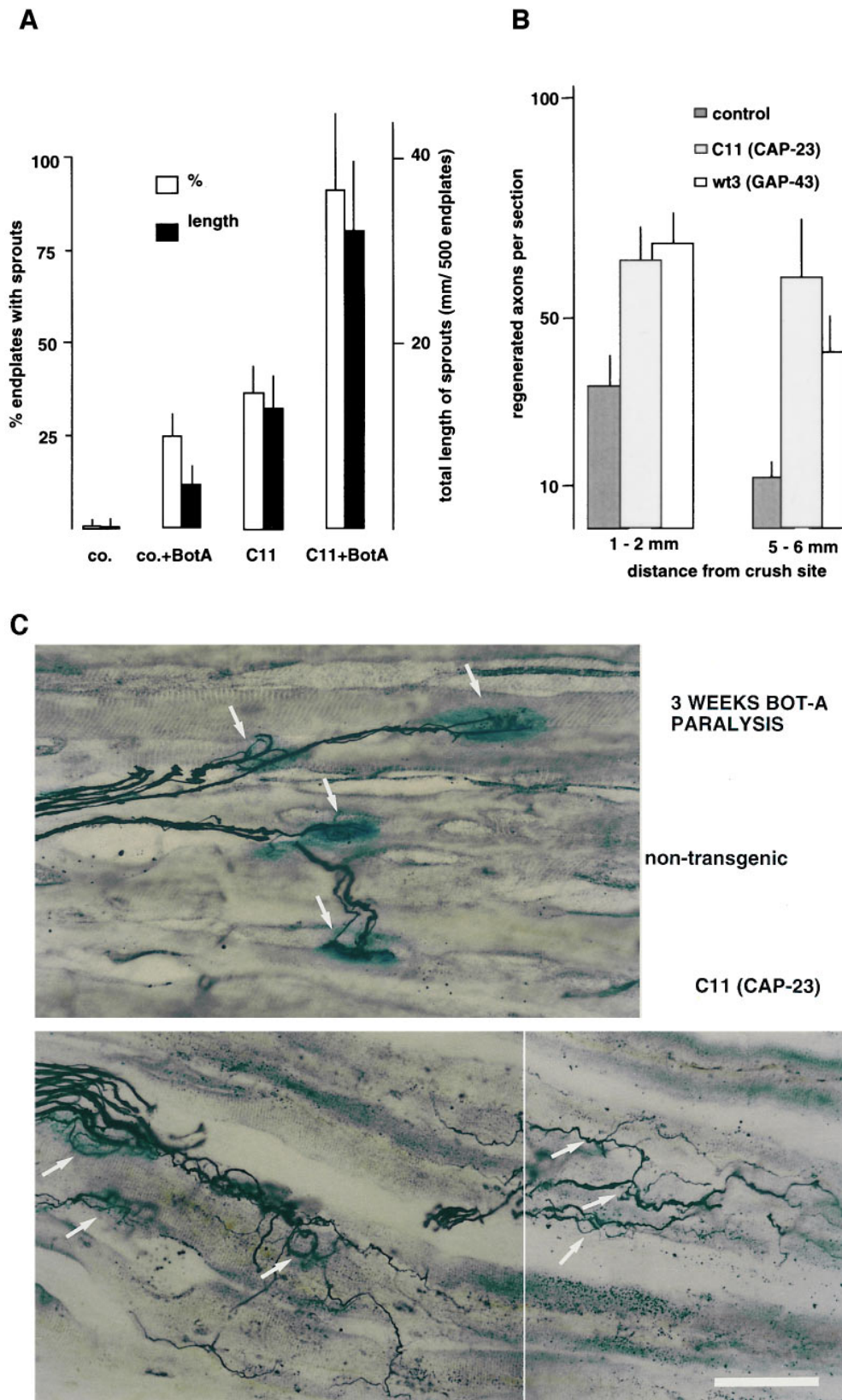
Figure 4. Potentiation of induced nerve sprouting in CAP-23–transgenic mice. All data from 5–8-wk-old mice; gluteus muscle or sciatic nerve. (*A*) Sprouting in untreated and Bot-A–paralyzed (8 d) muscle. Analysis as in Fig. 3 *C* (from which part of the data were replotted). $N = 5$. (*B*) Regenerative sprouting (at 64 h) distal from sciatic nerve crush. $N = 4$. (*C*) Ultraterminal nerve sprouting in chronically paralyzed (3 wk) muscle. Combined silver-esterase reaction; the plane of focus for the transgenic sample was selected to maximize visualization of sprouts (*arrows*, position of neuromuscular junctions; in part out of focus). Note dramatic extent of the sprouting reaction in the CAP-23(C11) mouse and very limited reaction in the nontransgenic mouse. These findings further support the conclusion that the presence of CAP-23 in motor nerves produces a true gain-of-function phenotype, leading to sustained potentiation of intramuscular nerve sprouting. Bar, 70 μm.

tative analysis of such preparations (see also Materials and Methods) yielded the following values: estimated areas within the outer synaptic boundaries were 1021 ± 125 μm^2 (control) and 962 ± 106 μm^2 (CAP-23[C11]); inside these outer synaptic regions, RITC–α-bungarotoxin–positive areas were 447 ± 86 μm^2 (control) and 668 ± 52 μm^2 (CAP-23[C11]). Significantly, no ectopic AChR clusters were detected in these experiments. Since the total muscle surface
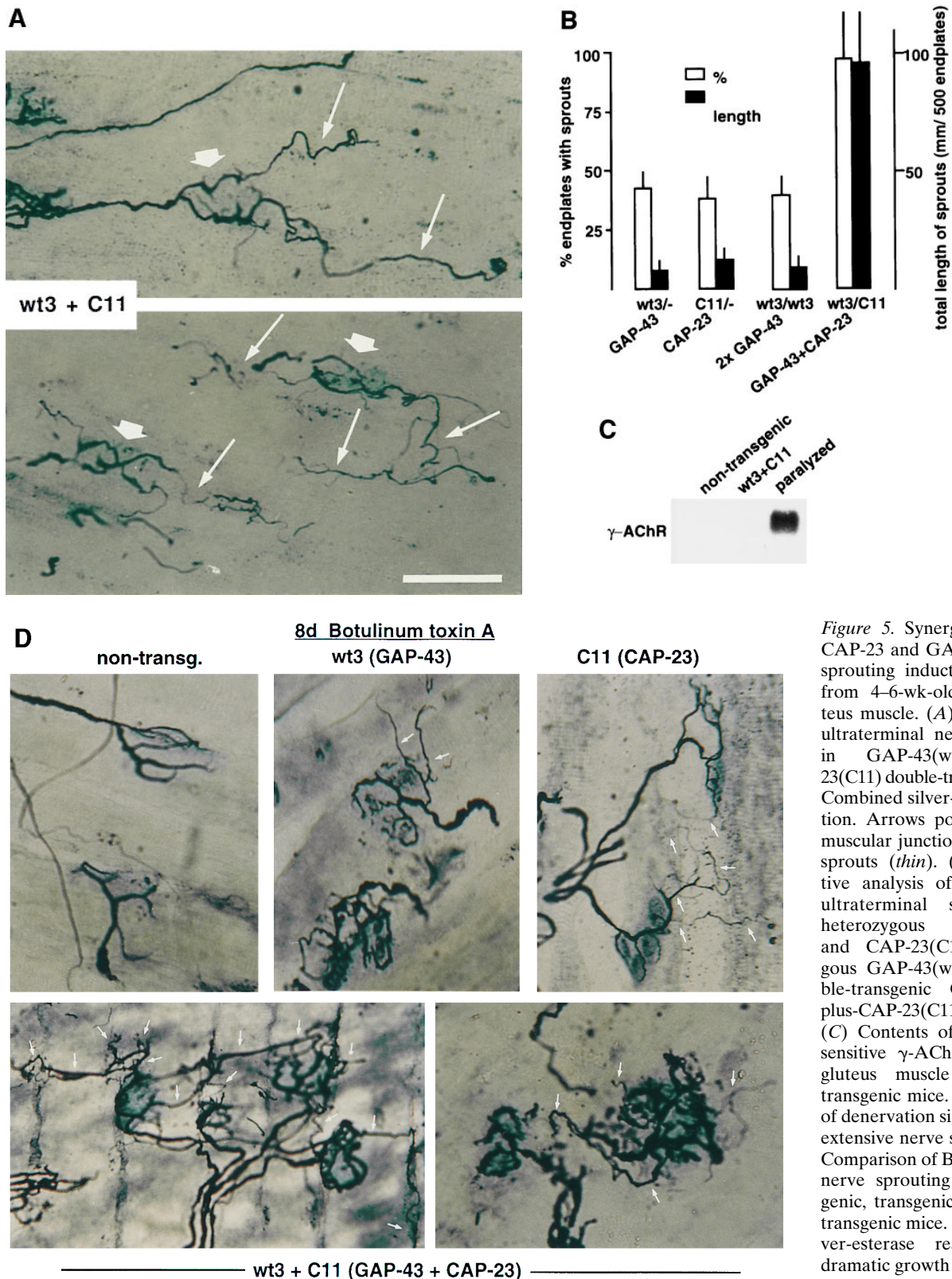
Figure 5. Synergism between CAP-23 and GAP-43 in nerve sprouting induction. All data from 4–6-wk-old mouse gluteus muscle. (*A*) Spontaneous ultraterminal nerve sprouting in GAP-43(wt3)-plus-CAP-23(C11) double-transgenic mice. Combined silver-esterase reaction. Arrows point to neuromuscular junctions (*thick*) and sprouts (*thin*). (*B*) Quantitative analysis of spontaneous ultraterminal sprouting in heterozygous GAP-43(wt3) and CAP-23(C11), homozygous GAP-43(wt3), and double-transgenic GAP-43(wt3)-plus-CAP-23(C11) mice. $N = 5$. (*C*) Contents of denervation-sensitive γ-AChR mRNA in gluteus muscle of double-transgenic mice. Note absence of denervation signs, in spite of extensive nerve sprouting. (*D*) Comparison of Bot-A–induced nerve sprouting in nontransgenic, transgenic, and double-transgenic mice. Combined silver-esterase reaction. Note dramatic growth at and behind neuromuscular junctions in double-transgenic mice. In nontransgenic mice, Bot-A induced elongation of most neuromuscular junctions and detectable nerve sprouting only at a subset of them. Some of the sprouts are indicated by arrows. Bar, 50 μm.

area contained within the outer outlines of the neuromuscular junction was not significantly different from control, and average muscle fiber diameters were also not altered in the transgenic mice (data not shown), these results suggest that the presence of the transgenes led to growth of nerve processes within the synaptic region, which then in turn induced postsynaptic structures underneath them. When AChR configurations and silver-stained nerve processes were compared, it became clear that although the nerve branching index at the synapse was elevated in the transgenic mice (Fig. 3 *D*; number of branch points per endplate), it failed to reveal the degree of complexity detected with RITC–α-bungarotoxin. This pointed to potential limitations in the effectiveness of the silver stain method to reveal nerve terminal structures at the neuromuscular junction. Because the silver precipitation method mainly reveals the presence of neurofilaments, a possible explanation for these discrepancies is that fine synaptic endings may have low contents of these neuronal cytoskeletal elements. To identify possible relations between the expansion in synaptic structure density detected in GAP-43– and CAP-23–overexpressing mice and synaptic activity, we analyzed AChR configurations in Bot-A–treated muscles. 8 d after treatment, in nontransgenic mice, paralyzing doses of Bot-A had a very modest effect on the length of AChR-positive synaptic branches, whereas an apparent expansion in total synaptic area (from 668 ± 52 μm^2 to 918 ± 78 μm^2) was detected in transgenic mice (Fig. 6 *B*). Significantly, Bot-A–induced paralysis did not induce a transgenic-type postsynaptic configuration in nontransgenic mice (Fig. 6 *B*; with respect to this last point, similar results were obtained upon 3-wk paralysis [data not shown]).

Multiple Activity-sensitive Mechanisms Promote Nerve Sprouting at the Neuromuscular Junction

What are the types of growth-inducing signals to which GAP-43– or CAP-23–expressing terminals respond? To begin to define relevant local mechanisms, we carried out a detailed analysis of Bot-A–induced sprouting. The purified Bot-A used for these studies induced detectable local signs of paralysis upon subcutaneous injection of 1 pg of toxin over the gluteus maximus or gastrocnemius muscle (toe-spreading reflex). A dose of 0.5 pg of toxin induced detectable paralysis signs in about one-fifth of the mice, and these signs were only detectable between 1 and 3 d after injection. If anything, transgenic mice were less sensitive to Bot-A–induced paralysis than nontransgenic ones. Finally, 0.3 pg of Bot-A induced no detectable signs of paralysis, and direct stimulation of the sciatic nerve 2 d after application of toxin doses below 0.5 pg elicited gastocnemius twitching undistinguishable from control (untreated animals). Therefore, although we cannot exclude that even very low toxin levels did induce paralysis at a subpopulation of neuromuscular synapses, these combined observations argue that local application of toxin doses lower than 0.3 pg failed to block nerve-induced muscle activation at most neuromuscular junctions. In agreement with these behavioral assessments, toxin doses lower than 1 pg failed to induce muscle wasting or activity-sensitive mRNAs in muscle (data not shown).

A dose-response analysis of Bot-A–induced sprouting revealed that in GAP-43– or CAP-23–overexpressing mice local growth reactions were already induced with 0.1 or even 0.05 pg of toxin, i.e., with doses substantially lower than those required to induce any signs of muscle paralysis (Fig. 7 *A*). Subparalyzing doses induced no detectable growth reactions in nontransgenic mice (Fig. 7 *A*). In transgenic mice, growth reactions in the absence of paralysis included an increase in endplate branching points and the appearance of numerous short ultraterminal sprouts. These reactions were already detectable 24 h after toxin application and developed to a maximal extent within 4–5 d (Fig. 7 *B*; similar results were obtained with CAP-23[C11] mice). Paralyzing doses of toxin induced similar reactions during the first 3 d, followed by pronounced extension of ultraterminal sprouts, starting about 4 d after toxin application (Fig. 7 *B*). Similar morphological responses were induced when neuromuscular transmission was abolished by blocking nerve action potentials with a tetrodotoxin cuff placed onto the sciatic nerve (Fig. 7 *C*), indicating that they were due to impairment of evoked transmitter release and not to effects more specifically linked to the activity of Bot-A (i.e., cleavage of nerve terminal SNAP-25). These results suggested that a mechanism linked to reduced calcium-induced transmitter release from motor nerves can induce local nerve growth in GAP-43– or CAP-23–expressing nerve terminals. To explore this possibility, we analyzed nerve sprouting upon local blockade of postsynaptic AChR activation with α-bungarotoxin. This paralysis-inducing paradigm led to stimulation of ultraterminal sprout elongation, starting 4–5 d after toxin application (Fig. 7 *C*). Significantly, however, stimulation of nerve branching at the neuromuscular junction (Fig. 7 *C*) and increased ultraterminal sprout formation (data not shown) were absent. When 0.5 μg of α-bungarotoxin were applied daily (for 3 d), thus subjecting the muscle to a more effective paralyzing protocol, these early sprouting responses were also not induced (data not shown). Finally, subparalyzing doses of α-bungarotoxin were without detectable effect. As discussed below, these results are consistent with the interpretation that reduced transmitter release induces local nerve growth through a direct mechanism that may be independent of the activation of muscle AChRs and that muscle paralysis leads to local conditions promoting the elongation of ultraterminal sprouts.

Discussion

We have shown that at mouse motor nerve synapses, both GAP-43 and the related protein CAP-23 are downregulated during the second postnatal week and are reinduced by nerve lesion. Like corresponding GAP-43–overexpressing mice (Aigner et al., 1995), CAP-23–overexpressing mice displayed spontaneous and greatly potentiated induced nerve sprouting at the adult neuromuscular junction. While GAP-43–induced sprouts were numerous, with prominent growth cone structures, in the presence of CAP-23 neuromuscular junctions displayed fewer, but longer sprouts with barely detectable growth cones. Sprouting and its transgene-specific features were greatly potentiated by treatments with Bot-A, and double-transgenic mice displayed profound potentiation of sprouting, with structural features reminiscent of both transgenes. These results
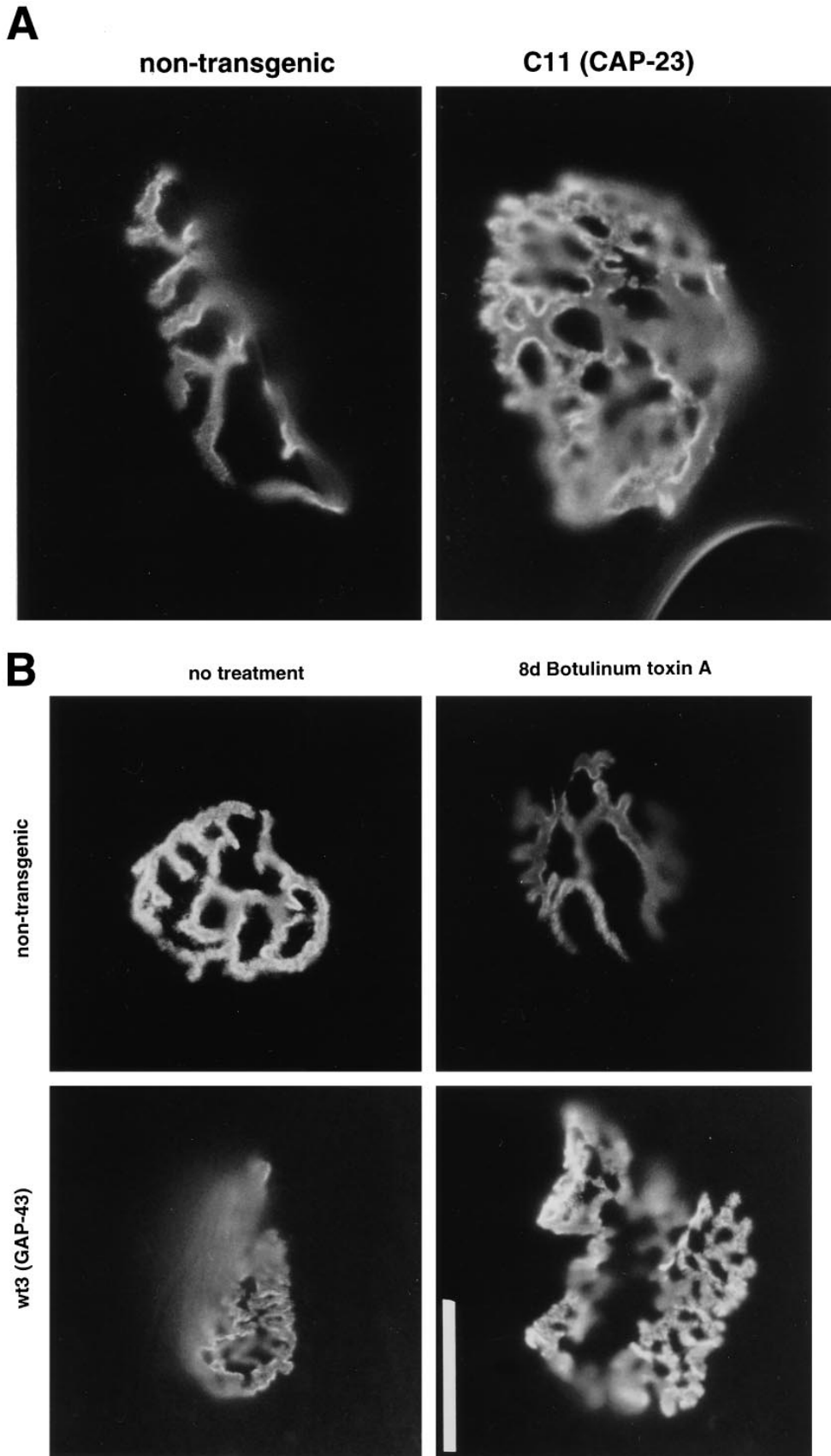
Figure 6. Increased neuromuscular synaptic areas in GAP-43– and CAP-23–overexpressing mice. RITC–α-bungarotoxin labeling of gluteus muscle fiber whole mounts (4–6-wk-old mice). (*A*) Representative examples of neuromuscular junction configurations in nontransgenic and CAP-23(C11) mice. Part of the nontransgenic endplate is out of focus, but the entire long-axis is in focus. Note dramatic increase in branching index and synaptic area in the transgenic mouse. In contrast, the external dimensions of the synaptic region did not differ significantly between transgenic and nontransgenic mice. (*B*) Representative examples of neuromuscular junction configurations in nontransgenic and GAP-43(wt3) mice, with and without Bot-A–induced paralysis. Note that paralysis did not induce features of transgenic endplates (e.g., high branching index) in nontransgenic mice. Bar: (*A*) 15 μm; (*B*) 29 μm.

A Bot-A dose-response (at 4 days)

Bot-A doses:
□ none
□ 0.05pg
□ 0.1pg
■ 1pg (paralyzing)

B Time course (wt3)

Days:
□ 0
□ 1
□ 2
□ 4
■ 8

C Sprout-inducing mechanisms (wt3)
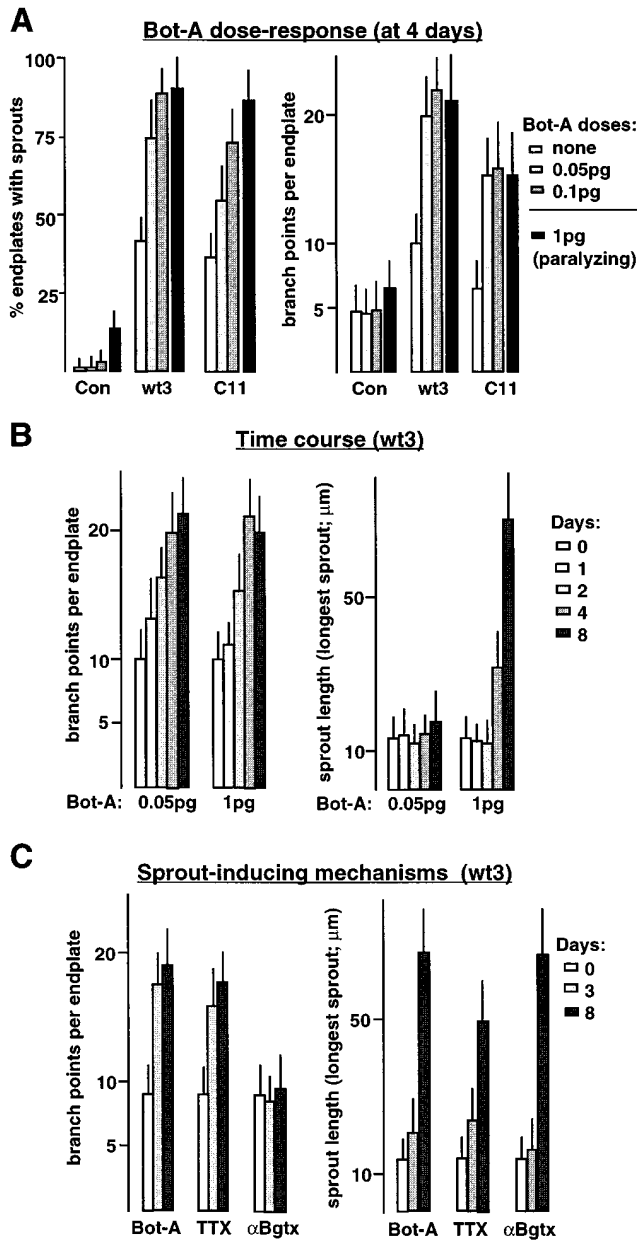
Days:
□ 0
□ 3
■ 8

Figure 7. GAP-43– and CAP-23–transgenic mice reveal a sprout-inducing mechanism sensitive to reduced transmitter release that may be independent of postsynaptic activation. Data from gluteus (*A* and *B*) or gastrocnemius (*C*) muscle of 4–7-wk-old mice. (*A*) Subparalyzing doses of Bot-A induce ultraterminal nerve sprouting and elevated contents of neurofilament-positive branch points at the neuromuscular junction. Nontransgenic (*Con*), GAP-43(wt3), and CAP-23(C11) mice were analyzed. 1 pg of Bot-A induced local paralysis in all mice, 0.5 pg failed to induce detectable paralysis signs in >80% of the mice, and 0.1 pg induced no detectable paralysis. Note that 0.05 pg of toxin was already highly effective in inducing sprouting and endplate branching (these two parameters were correlated) in GAP-43– and CAP-23–overexpressing mice. $N = 6$. (*B*) Time-course of Bot-A–induced nerve growth at the neuromuscular junction of GAP-43(wt3) mice. Sprout length: average length of the longest sprout per sprouting endplate. Note that subparalyzing doses of the toxin rapidly induced endplate branching (and the emergence of short ultraterminal sprouts; data not shown), whereas paralysis promoted sprout elongation with comparatively slow kinetics.

strongly support the hypothesis that mechanisms promoted by intrinsic neuronal components affect the potential for and pattern of local nerve growth.

Analysis of AChR distribution in whole-mount preparations of transgenic and nontransgenic mice with and without Bot-A treatment indicated that these growth mechanisms affect both extrasynaptic and synaptic structures. Finally, experiments with paralyzing and nonparalyzing doses of Bot-A, tetrodotoxin, and α-bungarotoxin revealed that at the neuromuscular junction, growth is activated by mechanisms that may directly sense reduced transmitter release independent of postsynaptic activity. Muscle paralysis, in addition, greatly promotes ultraterminal sprout elongation. As discussed below, a possible interpretation of these findings is that at the adult neuromuscular junction, intrinsic neuronal components determine competence and types of nerve growth, mechanisms sensitive to nerve activity, possibly involving terminal Schwann cells, promote nerve growth, and absence of postsynaptic activation leads to local conditions favoring sprout elongation.

Characteristics and Possible Mechanisms of GAP-43/ CAP-23–potentiated Sprouting

A main finding of this study is that the patterns of sprouting induced by GAP-43 or CAP-23 were different and that expression of both proteins in double-transgenic mice greatly potentiated nerve sprouting. The significance of these double-transgenic results is strengthened by the fact that, in analogous experiments, crossing of transgenic mice expressing different phosphorylation-site mutants of GAP-43, which did display subtle differences in nerve sprouting patterns (Aigner et al., 1995), did not produce potentiation of nerve sprouting (data not shown). The specific features of the sprouting detected in the presence of the different transgenes may have interesting biological implications. However, their interpretation will require a more detailed analysis of sprouting in these mice, in particular with respect to its dynamic and ultrastructural properties.

What may be the basis for the distinct and synergistic effects of GAP-43 and CAP-23 on local nerve growth? The molecular mechanisms affected by GAP-43 are still not clear. This cell membrane and cortical cytoskeleton–associated protein appears to be involved in a variety of dynamic processes at the cell periphery, including growth cone activity (Aigner and Caroni, 1995) and guidance (Strittmatter et al., 1995), and regulated secretion (Dekker et al., 1989; Imaizumi et al., 1995; Gambi et al., 1996). Potentially significant clues are its local abundance (up to 1% of growth cone and synaptosomal protein) and its interactions with calmodulin, PKC, and actin filaments (Benowitz and Routtenberg, 1987; Liu and Storm, 1990; Hens et al., 1993). In a recent study, we found that GAP-43, CAP-23, and a further abundant calmodulin- and actin-binding

---

$N = 4$. (*C*) Endplate nerve branching is induced by blockade of transmitter release in the presence of either Bot-A (1 pg) or tetrodotoxin (*TTX*), whereas paralyzing doses of α-bungarotoxin (*αBgtx*) failed to induce this reaction. In contrast, sprout elongation was induced by all paralysis-inducing protocols. These experiments were carried out in GAP-43(wt3) mice. $N = 4$.

PKC substrate, myristoylated alanine-rich C kinase substrate (MARCKS) (Aderem, 1995), share a number of unique properties, including accumulation at the same subplasmalemmal punctate structures and induction of the same characteristic spectrum of cell surface activities, including blebbing and filopodia formation (Wiederkehr, A., and P. Caroni, manuscript submitted for publication). Like GAP-43, MARCKS has been implicated in several processes involving cell surface dynamics, including cell migration, phagocytosis, and exocytosis (Aderem, 1995). Although they share certain biochemical and functional properties, GAP-43, CAP-23, and MARCKS are clearly regulated and targeted in very distinct manners (Skene and Virag, 1989; Allen and Aderem, 1995). GAP-43 and CAP-23 may thus affect similar local dynamic processes at the cell surface, and their differential targeting and regulatory properties may lead to complementary and synergistic effects (Wiederkehr, A., and P. Caroni, manuscript submitted for publication). A difficulty in defining the processes affected by these proteins is that very little is known about the mechanisms that translate local signaling into neurite outgrowth. However, when combined with the fact that both GAP-43 and MARCKS have been implicated in multiple motility processes at the cell surface, the results of this study are consistent with a role for GAP-43 and CAP-23 in the processes that link cortical cytoskeleton dynamics to membrane fusion. One possibility is that these proteins may shift a balance between stable membrane incorporation and rapidly reversible exo-/endocytosis (see e.g., Catsicas et al., 1994), thus favoring growth.

Mechanisms Regulating
GAP-43/CAP-23–mediated Plasticity

What local signaling mechanisms induce GAP-43/CAP-23–promoted growth? As shown by the results with the pre- and postsynaptically acting toxins, one of them appears to be mediated by reduced transmitter release and may not require postsynaptic nicotinic AChR activation. Although there is evidence suggesting that reduced transmitter release could signal back to the motor nerve (Hory-Lee and Frank, 1995), it seems very likely that the Schwann cells at the synapse (terminal-Schwann cells) mediate this growth-promoting signal. This is based on the fact that these cells can respond rapidly to changes in transmitter release (Reist and Smith, 1992; Georgiou et al., 1994) and that they appear to be causally involved in most if not all forms of nerve sprouting at the neuromuscular junction (Reynolds and Woolf, 1992; Son and Thompson, 1995). Out of a total of 22 transgenic lines, we never found any evidence of transgene expression in peripheral nerve or terminal-Schwann cells. To search for signs of terminal-Schwann cell activation in the transgenic mice, we analyzed endogenous GAP-43, GFAP, and low-affinity NGF receptor immunoreactivity on corresponding muscle sections. These experiments did not reveal obvious differences to nontransgenic mice (data not shown), suggesting that transgene expression may not have induced a reactive state in terminal-Schwann cells. It therefore seems most likely that, if they indeed mediate these growth reactions, terminal-Schwann cells in transgenic and nontransgenic mice respond in the same manner to reduced transmitter release, and that the presence of GAP-43 or CAP-23 affects the subsequent sprouting reaction. One puzzling observation was that within the same muscle, neuromuscular junctions with vigorous sprouting coexisted side-by-side with junctions that showed no detectable sprouting. This was obvious in all transgenic lines and in paralyzed muscle from nontransgenic mice. Transgene presence greatly enhanced both the extent of sprouting at single endplates and the proportion of endplates with sprouting. Although we currently have no explanation for this phenomenon, one possibility is that for sprouting to occur a threshold must be reached. This in turn may either be a property intrinsic to the nerve or may involve both the nerve and the terminal-Schwann cell.

Functional Implications of
GAP-43/CAP-23–mediated Plasticity

Structural changes at the neuromuscular junction of GAP-43– and CAP-23–overexpressing mice were not restricted to presynaptic structures. In the presence of either transgene, RITC–α-bungarotoxin–labeled synaptic structures displayed a pronounced increase in branching index and overall synaptic area. In contrast, we detected no extrajunctional AChR clusters in these muscles, suggesting that ultraterminal sprouts did not induce synaptic structures. Significantly, in nontransgenic mice, treatment with Bot-A failed to induce synaptic features resembling those in GAP-43– or CAP-23–overexpressing mice, regardless of the extent and duration of muscle paralysis. These results suggest that, within the synaptic region, presynaptic branching and growth due to the presence of GAP-43 or CAP-23 induced corresponding growth of synaptic structures in muscle. This phenomenon is probably related to nerve terminal outgrowth, the terminal branch elongation reaction detected in nontransgenic mice in response to Bot-A–induced paralysis (Pestronk and Drachman, 1978b).

In spite of these marked differences in overall synaptic structure, we found no evidence for major functional differences at the neuromuscular junction of transgenic and double-transgenic mice. Functional parameters not obviously different from control included the degree of muscle fiber polyinnervation and the amplitude and frequency of spontaneous miniature endplate potentials (data not shown). Although twofold and smaller changes in the frequency of spontaneous discharges may have gone undetected in our analysis, the results suggest that major alterations in overall synaptic structure were not accompanied by obvious changes in synaptic function. This finding is consistent with the evidence from other studies indicating that at the neuromuscular junction, structural plasticity does not necessarily lead to corresponding functional plasticity (Tsujimoto et al., 1990; Stewart et al., 1996). As suggested recently, this may reflect homeostasis of synaptic transmission (Stewart et al., 1996), possibly involving corresponding changes in active zone density (Budnik et al., 1990; Tsujimoto et al., 1990; Woytowicz et al., 1994; Stewart et al., 1996). These questions will be adressed by an analysis of ultrastructural parameters at the neuromuscular junction of the transgenic mice.

Finally, because of the ease and resolution of the histological analysis and the possibilities for targeted experimental manipulations, we focussed our analysis on the neu-

romuscular junction. However, because of the restricted and distinct expression of endogenous CAP-23 and GAP-43 in the adult nervous system and the widespread expression of CAP-23 and GAP-43 in the transgenic mice, one may predict similar effects on local nerve sprouting also in the central nervous system. In several transgenic lines overexpressing GAP-43, we detected pronounced sprouting of zinc-containing mossy fiber terminals into the pyramidal cell layer of CA3 (Aigner et al., 1995). In spite of substantial transgene expression in dentate gyrus granule cells, none of the CAP-23–overexpressing lines displayed comparable massive sprouting reactions. These findings further argue for the existence of significant functional differences between GAP-43 and CAP-23. However, because it is technically impossible to resolve the terminal arbors of single neurons in these experiments, the informative value of these data is limited, and spontaneous nerve sprouting in the adult central nervous system will have to be analyzed at a much higher resolution.

In conclusion, a substantial amount of experimental evidence supports the view that terminal arborization and alterations in synaptic structures are involved in activity-sensitive plasticity during development and in the adult. The results of this study now suggest that differential expression of intrinsic neuronal components affects the extent and pattern of activity-sensitive structural plasticity in the nervous system. The availability of transgenic mice with greatly elevated potential for structural plasticity should provide a valuable experimental system to study the regulation and roles of structural alterations for the normal function of the adult nervous system.

References

Aderem, A. 1995. The MARCKS family of protein kinase-C substrates. *Biochem. Soc. Trans.* 23:587–591.

Aigner, L., and P. Caroni. 1995. Absence of persistent spreading, branching, and adhesion in GAP-43-depleted growth cones. *J. Cell Biol.* 128:647–660.

Aigner, L., S. Arber, J.P. Kapfhammer, T. Laux, C. Schneider, F. Botteri, H.-R. Brenner, and P. Caroni. 1995. Overexpression of the neural growth-associated protein GAP-43 induces nerve sprouting in the adult nervous system of transgenic mice. *Cell.* 83:269–278.

Allen, L.-A. H., and A. Aderem. 1995. Protein kinase C regulates MARCKS cycling between the plasma membrane and lysosomes in fibroblasts. *EMBO (Eur. Mol. Biol. Organ.) J.* 14:1109–1121.

Arber, S., and P. Caroni. 1995. Thrombospondin-4, an extracellular matrix protein expressed in the developing and adult nervous system promotes neurite outgrowth. *J. Cell Biol.* 131:1083–1094.

Arber, S., G. Halder, and P. Caroni. 1994. Muscle LIM protein, a novel positive regulator of myogenesis, promotes myogenic differentiation. *Cell.* 79:221–231.

Bailey, C.H., C. Alberini, M. Ghirardi, and E.R. Kandel. 1994. Molecular and structural changes underlying long-term memory storage in Aplysia. *Adv. Second Messenger Phosphoprotein Res.* 29:529–544.

Benowitz, L.I., and A. Routtenberg. 1987. A membrane phosphoprotein associated with neural development, axonal regeneration, phospholipid metabolism, and synaptic plasticity. *Trends Neurosci.* 10:527–531.

Brown, M.C. 1984. Sprouting of motor nerves in adult muscle: a recapitulation ontogeny. *Trends Neurosci.* 7:10–14.

Budnik, V., Y. Zhong, and C.-W. Wu. 1990. Morphological plasticity of motor axons in Drosophila mutants with altered excitability. *J. Neurosci.* 10:3754–3768.

Caroni, P. 1997. Overexpression of growth-associated proteins in the neurons of adult transgenic mice. *J. Neurosci. Methods.* In press.

Caroni, P., and M. Becker. 1992. The downregulation of growth-associated proteins in motoneurons at the onset of synapse elimination is controlled by muscle activity and IGF1. *J. Neurosci.* 12:3849–3861.

Caroni, P., C. Schneider, M.C. Kiefer, and J. Zapf. 1994. Role of muscle insulin-like growth factors in nerve sprouting: suppression of terminal sprouting in paralyzed muscle by IGF-binding protein 4. *J. Cell Biol.* 125:893–902.

Catsicas, S., G. Grenningloh, and E.M. Pich. 1994. Nerve-terminal proteins: to fuse to learn. *Trends Neurosci.* 17:368–373.

Darian-Smith, C., and C.D. Gilbert. 1994. Axonal sprouting accompanies functional reorganization in adult cat striate cortex. *Nature (Lond.).* 368:737–740.

Das, A., and C.D. Gilbert. 1995. Long-range horizontal connections and their role in cortical reorganization revealed by optical recording of cat primary visual cortex. *Nature (Lond.).* 375:780–784.

Dekker, L.V., P.N.E. DeGraan, A.B. Oestreicher, D.H.G. Versteeg, and W.H. Gispen. 1989. Inhibition of noradrenaline release by antibodies to B-50(GAP-43). *Nature (Lond.).* 342:74–76.

Gambi, C., M.C. Waage, R.G. Allen, and L. Baizer. 1996. Growth-associated protein-43 (GAP-43) facilitates peptide hormone secretion in mouse anterior pituitary AtT-20 cells. *J. Biol. Chem.* 271:10023–10028.

Georgiou, J., R. Robitaille, W.S. Trimble, and M.P. Charlton. 1994. Synaptic regulation of glial protein expression in vivo. *Neuron.* 12:445–455.

Hens, J.J.H., F. Benfenati, H.B. Nielander, F. Valtorta, W.H. Gispen, and P.N.E. DeGraan. 1993. B-50/GAP-43 binds to actin filaments without affecting actin polymerization and filament organization. *J. Neurochem.* 61:1530–1533.

Hory-Lee, F., and E. Frank. 1995. The nicotinic blocking agents d-tubocurare and α-bungarotoxin save motoneurons from naturally occurring death in the absence of neuromuscular blockade. *J. Neurosci.* 15:6453–6460.

Imaizumi, K., T. Katoh, M. Tsuda, T. Takagi, and H. Kiyama. 1995. GAP-43 mRNA suppression by the rybozyme in PC12 cells and inhibition of evoked release of dopamine. *Mol. Brain Res.* 32:338–341.

Liu, Y., and D.R. Storm. 1990. Regulation of free calmodulin levels by neuromodulin: neuron growth and regeneration. *Trends Pharmacol. Sci.* 11:107–111.

Maekawa, S., M. Maekawa, S. Hattori, and S. Nakamura. 1993. Purification and molecular cloning of a novel acidic calmodulin-binding protein from rat brain. *J. Biol. Chem.* 268:13703–13709.

Maekawa, S., H. Murafushi, and S. Nakamura. 1994. Inhibitory effect of calmodulin on phosphorylation of NAP-22 with protein kinase C. *J. Biol. Chem.* 269:19462–19465.

Meiri, K.F., and P.R. Gordon-Weeks. 1990. GAP-43 in growth cones is associated with areas of membrane that are tightly bound to substrate and is a component of a membrane skeleton subcellular fraction. *J. Neurosci.* 10:256–266.

Moss, D.J., P. Fernyhough, K. Chapman, L. Baizer, D. Bray, and T. Allsopp. 1990. Chicken growth-associated protein GAP-43 is tightly bound to the actin-rich neuronal membrane skeleton. *J. Neurochem.* 54:729–736.

Pestronk, A., and D.B. Drachman. 1978a. A new stain for quantitative measurement of sprouting at neuromuscular junctions. *Muscle Nerve.* 1:70–74.

Pestronk, A., and D.B. Drachman. 1978b. Motor nerve sprouting and acetylcholine receptors. *Science (Wash. DC).* 199:1223–1225.

Reist, N.E., and S.J. Smith. 1992. Neurally evoked calcium transients in terminal Schwann cells at the neuromuscular junction. *Proc. Natl. Acad. Sci. USA.* 89:7625–7629.

Reynolds, M.L., and C.J. Woolf. 1992. Terminal Schwann cells elaborate extensive processes following denervation of the motor endplate. *J. Neurocytol.* 21:50–66.

Schaeren-Wiemers, N., and A. Gerfin-Moser. 1993. A single protocol to detect transcripts of various types of expression levels in neural tissue and cultured cells: in situ hybrdization using digoxigenin-labeled cRNA probes. *Histochemistry.* 100:431–440.

Skene, J.H.P. 1989. Axonal growth-associated proteins. *Annu. Rev. Neurosci.* 12:127–156.

Skene, J.H.P., and I. Virag. 1989. Posttranslational membrane attachment and dynamic fatty acylation of a neuronal growth cone protein, GAP-43. *J. Cell Biol.* 108:613–624.

Son, Y.-J., and W.J. Thompson. 1995. Nerve sprouting in muscle is induced and guided by processes extended by Schwann cells. *Neuron.* 14:133–141.

Stewart, B.A., C.M. Schuster, C.S. Goodman, and H.L. Atwood. 1996. Homeostasis of synaptic transmission in Drosophila with genetically altered nerve terminal morphology. *J. Neurosci.* 16:3877–3886.

Strittmatter, S.M., C. Fankhauser, P.L. Huang, H. Mashimo, and M.C. Fishman. 1995. Neuronal pathfinding is abnormal in mice lacking the neuronal growth cone protein GAP-43. *Cell.* 80:445–452.

Tsujimoto, T., M. Umemiya, and M. Kuno. 1990. Terminal sprouting is not responsible for enhanced transmitter release at disused neuromuscular junctions of the rat. *J. Neurosci.* 10:2059–2065.

Vidal, M., R. Morris, F. Grosveld, and E. Spanopoulou. 1990. Tissue-specific control elements of the Thy-1 gene. *EMBO (Eur. Mol. Biol. Organ.) J.* 9:833–840.

Widmer, F., and P. Caroni. 1990. Identification, localization, and primary structure of CAP-23, a particle-bound cytosolic protein of early development. *J. Cell Biol.* 111:3035–3047.

Witzemann, V., H.R. Brenner, and B. Sakmann. 1991. Neural factors regulate AChR subunit mRNAs at rat neuromuscular synapses. *J. Cell Biol.* 114:125–141.

Woolf, C.J., P. Shortland, and R.E. Coggeshall. 1992. Peripheral nerve injury triggers central sprouting of myelinated afferents. *Nature (Lond.).* 355:75–78.

Woytowicz, M., L. Marin, and H.L. Atwood. 1994. Activity-induced changes in synaptic release sites at the crayfish neuromuscular junction. *J. Neurosci.* 14:3688–3703.